A balanced translocation in Kallmann Syndrome implicates a long noncoding RNA, RMST, as a GnRH neuronal regulator.

Maria Stamou[1]*, Shi-Yan Ng[2]*, Harrison Brand[3,4,5], Harold Wang [3], Lacey Plummer[1], Lyle Best[6,7], Steven Havlicek[9], Martin Hibberd[8,9], Chiea Chuen Khor[9], James Gusella[3] , Ravikumar Balasubramanian[1], Michael Talkowski[3,4,5], Lawrence W. Stanton [9,10]*, William F. Crowley, Jr[1,3]*

*Contributed equally

1. Harvard Reproductive Endocrine Science Center, Mass. General Hospital, Boston

2. Institute of Molecular & Cell Biology, 61 Biopolis Dr., Singapore 138673

3. Center for Genomic Medicine, Mass. General Hospital, Boston

4. Neurology, Psychiatry, & Pathology Departments, Mass. General Hospital, Boston

5. Program in Medical & Population Genetics, Broad Institute, Cambridge, MA

6. Turtle Mountain Community College, Belcourt, ND

7. Family Medicine Department, U. of No. Dakota, Grand Forks, ND

8. London School of Hygiene & Tropical Medicine, Keppel Street, London, WC1E 7HT

9. Genome Institute of Singapore

10. Current address: Qatar Biomedical Research Institute, Doha, Qatar

***Corresponding Author*:**

William F. Crowley, Jr., M.D.

Center for Genomic Medicine CPZN-6.6312 - 185 Cambridge Street, Boston, MA 02114

email: wcrowley@mgh.harvard.edu

Grant numbers: Funded by NIH grants P50HD028138, R01HD081256, GM061354 and K99DE026824 and Singapore's Agency for Science, Technology and Research. Dr. Talkowski was supported as the Desmond and Ann Heathwood MGH Research Scholar. Dr. Stamou was funded by the Daland Fellowship of the American Philosophical Society. The DGAP project was supported by GM061354.

Disclosure Summary: The authors have nothing to disclose.

Abstract

Context: Kallmann Syndrome (KS), is a rare, genetically heterogeneous Mendelian disorder in which structural defects in KS patients have helped define the genetic architecture of GnRH neuronal development in this condition.

Objective: Examine the functional role a novel structural defect affecting a long noncoding RNA (lncRNA), *RMST*, found in a KS patient.

Design: Whole genome sequencing (WGS), induced pluripotent stem cells (IPSC) and derived neural crest cells (NCC) from the KS patient were contrasted with controls. **Setting**: The Harvard Reproductive Sciences Center, MGH Center for Genomic Medicine and Singapore Genome Institute.

Patient: A KS patient with a unique translocation, t(7;12)(q22;q24).

Interventions/Main Outcome Measure/ Results: A novel translocation was detected affecting the lncRNA, *RMST*, on chromosome 12 in the absence of any other KS mutations. Compared to controls, the patient's iPSC and NCC provided functional information regarding *RMST*. Whereas *RMST* expression increased during NCC differentiation in controls, it was substantially reduced in the KS patient's NCC co-incident with abrogated NCC morphological development and abnormal expression of several 'downstream' genes essential for GnRH ontogeny (*SOX2, PAX3, CHD7, TUBB3 & MKRN3*). Additionally, an intronic SNP in *RMST* was significantly implicated in a GWAS associated with age of menarche.

Conclusions: A novel deletion in RMST implicates the loss of function of a lncRNA as a unique cause of KS and suggests it plays a critical role in the ontogeny of GnRH neurons and puberty.

Introduction

The hypothalamic peptide, **G**o**n**adotropin **R**eleasing **H**ormone (GnRH), is a prime mover of sexual maturation in mammals [1]. Human genetics has identified mutations in several genes that cause Isolated GnRH deficiency (IGD), a rare Mendelian disorder [2] manifested by abnormal puberty, hypogonadotropism and infertility [2]. Kallmann Syndrome (KS) is a phenotypic subset of IGD defined by the association of IGD with anosmia. Discoveries of nearly 20 mutated genes in KS patients have begun to define an emerging genetic architecture governing GnRH neuronal development

[3-8].

Following early fate specification as GnRH cells, GnRH precursor cells co-migrate with their olfactory companions into the CNS apparently utilizing common guidance mechanism(s) shared with olfactory axons. These still-maturing GnRH neurons permeate the porous cribriform plate guided via as yet unknown genes on the journey to their final hypothalamic destination from which they oversee the control of the reproductive axis in all mammals [9, 10]. During these complex developmental processes, GnRH neurons mature and expand their numbers, eventually giving rise to a population of ~10,000 functioning GnRH neurons in the hypothalamus that ultimately govern human reproduction [3, 10].

Critical biological clues regarding the genetic components that control these basic developmental processes have been provided by the discovery of several distinct structural genomic variations in KS patients. An Xp22.3 contiguous gene syndrome established anosmia 1- *ANOS1* (previously known as Kallmann 1- *KAL1*) as the first KS gene [9, 11-13]. Chr8p11 deletions in KS patients with hereditary spherocytosis [14]

identified fibroblast growth factor receptor 1- *FGFR1* as the first autosomal dominant KS gene [15]. Similarly, balanced chromosomal rearrangements on chr10 and chr12 identified WD Repeat Domain 11- *WDR11* as a cause of KS [16] and a heterozygous deletion revealed semaphoring 1- *SEMA3A* as another causal KS gene [17]. The studying such informative structural events has been particularly limited by their rarity and the utilization of traditional human genetic methodologies.

We have used next generation sequencing (NGS) in a KS patient previously reported to harbor a "balanced" t(7;12) chromosomal translocation. NGS can resolve structural defects to the single base pair level and thus reveal ever subtler defects in unknown disease-causing genes [18-20]. Using NGS, we revealed a previously unrecognized breakage on Ch12 that disrupted *RMST,* a gene not previously linked to IGD. RMST is a lncRNA that has been previously shown to regulate neurogenesis through its direct binding to the transcription factor Sox2 [21]. To assess if the identified defect in RMST in our patient contributes to KS, we performed functional studies using NCC generated from healthy control and patient-derived iPSC. These studies demonstrate novel developmental impacts associated with the loss of function of *RMST* in GnRH neuronal and NCC development.

Materials and Methods

Long insert whole genome sequencing (LiWGS) was performed on the KS patient's cell lines/DNA samples that were obtained from the NIGMS Human Genetic Cell Repository at the Coriell Institute and delineated the breakpoints of a previously identified apparently

balanced *de novo* translocation t(7;12)(q22;q24) [20, 22, 23] as previously described [19, 24-28] (**Figure 1**) that were validated by Sanger sequencing.

Whole Exome Sequencing (WES) was performed on the Broad Institute's Sequencing Platform and rare sequence variants (RSVs) in the 35 known IGD genes were sought (**Table S1[29])**.

Targeted Sequencing of potential *RMST* disruption in IGD Cohort: The *RMST* locus on chromosome 12 was captured end to end (introns and exons included) from hg19/b37 genomic coordinates 12:97856799 to 97929544 using the Roche Nimblegen SeqCap Easy Probe kit requiring that >95% of the *RMST* locus target bases be covered at least 10X.

Copy number variations (CNVs): A cohort of IGD samples were sequenced for CNVs using the iPsychCNV pipeline [30] from a cohort of 1,386 patients with genotypes from the Illumina PsychChip SNP array [31] and annotated against genecode_v19 [32].

Generation of pluripotent stem cells from proband/controls and differentiation of KS and wild-type iPSCs into neural crest cells (NCC): To test *RMST* expression in neural crest cells, the previously published stepwise differentiation of human pluripotent stem cells (hPSCs) to multipotent NC cells was used [33]. The resulting iPSCs were then treated for 11 days with the Wnt agonist (CHIR99021) under dual-SMAD inhibition for the first 4 days [34]. Efficiency of NCC induction was monitored based on SOX10 immunostaining, which marks early multipotent NC stem cells.

RMST expression in iPSCs and NCCs: Expression of *RMST* and all genes presented in **Figures 2, 3A & B** was quantified via qRT-PCR primers previously described [21].

SOX10 RNA-immunoprecipitation (RIP) (Day 21 NCC lysates): RIP was performed as described [21] on Day 11 NCs cells harvested in RIP buffer. Cells lysates were pre-cleared with Protein G magnetic beads before incubating with specific antibodies against *SOX10* or an IgG control. For each assay, 5 mg of antibodies was used, incubated with pre-cleared lysate at RT for 4 hours, and incubated with protein G magnetic beads for 2 hours. The resulting bound proteins were washed X3 in RIP buffer and eluted in Trizol reagent for RNA extraction.

ChIP-Seq Analysis: Chip- Seq analysis was performed to identify SOX2 binding sites in human neural stem cell lines as previously described [21]. In brief, redundant reads that could result from the over-amplification of ChIP DNA were removed and peak enrichment then calculated relative to the genome background. A threshold of $p = 10^{-5}$ was used to call significant peaks. An ‘‘input’’ sample was also included to eliminate nonrandom enrichment [35]. To filter for high-confidence ChIP-seq peaks, the difference between the *SOX2* libraries and input mapped reads were plotted vs. random *SOX2* peaks. Peaks with a greater peak height in comparison to random peaks were then selected. For motif discovery, the HOMER 4.1 algorithm [36] was applied to each set of ChIP-seq libraries for *de novo* binding motif discovery and known motif analysis with default parameters. All significant peaks were used for motif analysis in both sets of *SOX2* ChIP-seq experiments. The HOMER 4.1 software annotated the peaks using the hg18 genome assembly RefSeq genes transcription start site (defined from -1 kb to +100 bp), transcription termination site (by default defined from -100 bp to +1 kb), exons, 50 UTR, 30 UTR, introns, and intergenic regions.

Statistical analysis: All assays were performed in 3 independent experiments (biological replicates). Student’s t test was performed to assess statistical significance. Throughout

the manuscript, * denotes p < 0.05, ** denotes p < 0.01 and *** denotes p < 0.001. To test for excess of rare variants, IGD cases were compared to control cohorts we utilized the gnomAD database[37] using Fisher's exact test. *P* < .05 was considered significant.

Study approval: Approval from the tribal and Indian Health Service IRB and the MGH IRBs were obtained.

Results:

A Kallmann Syndrome patient with a *de novo* chromosomal translocation

A Native American (Chippewa/French) man diagnosed with Kallmann Syndrome (KS) presented at age 22 with a prepubertal status, hypogonadotropism and anosmia, unfused epiphyses, shortened metacarpals with clubbed distal ends, a sharply outlined occipital region, and delayed mental development confirmed by formal testing [20, 22, 23]. He never underwent treatment for his hypogonadism. By age 44, he had developed hypertension and Type II Diabetes. He was 175 cm tall, weighed 89.5 kg, had a span of 156 cm (difficult with prior orthopedic surgeries implying skeletal dysplasia) and an upper/lower segment ratio of 0.68. He remained undervirilized with no axillary and sparse pubic hair. His penis was underdeveloped and testes were prepubertal at <4ml. He had no neurologic deficits. He was the oldest of 6 full siblings (5 female and 1 male) and 3 half siblings (2 male and 1 female), all without evidence of KS or other reproductive or skeletal disorders. Laboratory confirmed hypogonadotropic hypogonadism and a pyelogram showed two normal kidneys. His initial karyotype revealed a reciprocal translocation (7;12)(q22;q24) that was absent in both parents and an additional, paternally inherited pericentric polymorphic inversion (9)(p12q13) which is a common variation [38-42].

Precise mapping of chromosomal breakpoints.

No genes previously associated with KS mapped to the breakpoints on Ch7 and Ch12 that were observed in this patient. Therefore, we used NGS to more accurately determine the genetic variations of this patient. Applying long insert whole genome sequencing (LiWGS) (cf. **Methods** &. **Figure 1**) we precisely determined the genomic breakpoints at t(7;12)(q21.13,q23.1). This sequencing revealed a 2 bp deletion on Chr12 that disrupted intron 2 of the longest transcript of a previously identified lncRNA [AK056164 (2.5 kb); chr12:97,860,651-97,860,653] of the Rhabdomyosarcoma 2 Associated Transcript (OMIM#607045)], *RMST*. The disruption led the gene to span into two different chromosomes, implying the complete disruption of this lncRNA and/or separation of the second piece of gene from its regulatory region. The other breakpoint on Ch7 did not disrupt any annotated gene [43]. Neither breakpoint spans known DNase I hypersensitivity sites nor disrupts any open reading frames of *RMST*. The Database of Genomic Variants revealed few duplications spanning this region and extremely rare microdeletions were reported by the 1,000 Genome Project [44]. Additional searches of ~13,991 controls [19] confirmed the absence of any copy number variations (CNVs) spanning this region.

We next performed whole exome sequencing (WES) of the proband to identify any coding variants. WES revealed a rare missense variant in the gene of leptin receptor ,*LEPR:* p.V658I predicted to be benign by Polyphen [45] and SiFT [46] with a minor allele frequency (MAF) [37] of 0.0001733 in ExAC and a MAF of 0.001732 in ExAC's African

subpopulation. No loss-of-function (LoF) rare sequencing variants (RSVs) in any of the 35 known isolated GnRH deficiency (IGD) genes existed (cf. **Table S1[29])**. Thus, the unique *de novo* disruption in *RMST* was the only genetic abnormality evident by LiWGS and WES in the genome of this KS patient.

Sequencing the *RMST* locus in additional IGD patients

Given the finding of a novel *RMST* breakage in the proband, we searched for RMST genetic variations in a cohort of 622 IGD individuals (292 KS and 330 nIHH). For each patient DNA sample, the *RMST* locus was captured with primers and sequenced with at least 10X coverage. A total of 17 RSVs in *RMST* were detected (13 KS and 18 nIHH), all of which were unique or had a MAF frequency <1% [37] (**Table 1)**. One KS patient carried 3 RSVs in *RMST*. No rare non-coding exonic homozygous RSVs in *RMST* exist in GnomAD. Ethnicity-based burden testing was performed to test for statistical excess of RSVs in IGD probands vs. ethnically matched controls (**Table 2)**. An excess of such RSVs was seen in Caucasian/non-Finish Europeans and African Americans control cohorts whereas Asian IGD patients showed a non-significant excess compared to Asian controls [47]. No other structural variants (CNVs) at the *RMST* site of any others were found in 1,386 IGD probands.

***RMST* expression in cell-based models of neural crest cell development**

RMST is highly expressed in the murine hypothalamus, at lower levels in whole brain, and is undetectable in mature (GT1-7) and immature (GN11) murine isogenic GnRH-

producing cell lines (data not shown). *RMST* expression has previously been demonstrated to be critical for neuronal development [21]. Hence, its role in the development of specific subsets of neurons derived from neural crest cells (i.e. those presumably contributing to GnRH neurogenesis) was examined. To address this issue, an *in vitro* model of NCC development was developed to begin to define *RMST*'s role in neurogenesis in the patient vs control (N=6) cell lines.

Using episomal reprogramming vectors, patient-specific, induced pluripotent stem cells (iPSC) were generated from lymphoblastoid cells derived from the proband. These patient-derived iPSC (KS1-iPSC) were confirmed to be pluripotent by expression of Oct4, Nanog, Sox2, and Tra1-81 (pluripotency markers) and their ability to generate all 3 germ layers by *in vitro* differentiation (**Figure S1A** & **S1B[29]**). The presence of t(7;12) chromosomal translocation was confirmed in KS1-iPSC by PCR amplification (**Figure S1C[29])** and DNA sequencing (data not shown); the *RMST* breakpoints were identical to those of the patient's DNA. Neural crest cells (NCC) were subsequently derived from the KS1-iPSC and healthy control iPSC (CTS-iPSC) by directed differentiation using established protocols involving the inhibition of BMP, TGF-β, and WNT signaling pathways. Differentiation was assessed by expression of Sox10, a marker of early, multipotent NC stem cells.

While *RMST* expression was detected in both the KS1-iPSC and healthy CTS- iPSCs, the KS1-iPSCs had significantly decreased expression of all *RMST* transcripts (~6%-18% vs. healthy iPSCs; $p < 0.0018$) (**Figure 2)**. During NCC development, *RMST* transcripts increased for control iPSCs as differentiation progressed coincident with the appearance of known neural crest markers, p75NGFR and AP2a (**Figure S2[29])**. In contrast, *RMST* transcripts in KS1-iPSC during this same period following NCC differentiation (Day 11)

showed significant reductions in all isoforms of *RMST* (*AK056164, AF429305 and AF429306*) that were <10% of healthy NCC ($p < 0.0001$) (**Figure 3A**) confirming reduced *RMST* expression in the patient's iPSC and NCC.

RMST binds to SOX10 in iPSC-derived neural crest cells

RMST has been shown to interact directly with *SOX2* during neurogenesis. Therefore, we explored whether *RMST* interacts directly with *SOX10*. Sox10-specific antibodies were used in RNA immunoprecipitation (RIP) experiments in NCC derived in vitro from iPSC. Robust enrichment of *RMST* was observed in *SOX10* RIP (Figure 4). As both *RMST* and *SOX2* are essential for neuronal development, it is plausible that *RMST-SOX10* interactions are similarly critical for NCC differentiation. To confirm that *RMST* interactions with *SOX10* and *SOX2* are similar, both KS and healthy iPSCs were exposed to NCC differentiation conditions and the *SOX10*-expression in NCC cells quantified. The efficiency of NCC differentiation in healthy iPSCs was 10% vs only 2% of the KS1 iPSCs that became *SOX10*+ NCC cells (cf. **Figure 5**).

Evidence of Direct *RMST-SOX2* Interactions: Using Chip-Seq analysis [21] and siRNA depletion of *RMST* in neuronal stem cells, *SOX2* binding sites were assessed at 35 known IGD genes. Of the 15 IGD genes containing a *SOX2* binding site (**Table 3)**, *RMST* deletion induced loss of occupancies in 12/15, several of which are known major and/or candidate IGD genes affecting sexual maturation including: *FGFR1, TAC3, NROB1, LEPR, SOX10,*

RNF216, OTUD4, FEZF1, MKRN3, IL17RD) and *DUSP6*. Intriguingly, *SOX2* binding sites on *TACR3, TUBB3* and *FLRT3* were not altered upon deletion of *RMST* and, in *PROKR2,* a novel SOX2 binding site was acquired upon *RMST* depletion.

Effect of *RMST* LoF on downstream target genes: Previous depletion of *RMST* by siRNA in neural stem cell lines decreased the levels of the known IGD- associated genes *CHD7, TUBB3* & *SEMA3A* and increased *MKRN3* [21]. To determine these effects of our patient's *RMST* depletion on these same IGD genes, their levels were measured in the KS1 and control NCC on Days 11 and 21 of differentiation (**Figure 3A).** At Day 11, KS1 cells expressed reduced levels of *SOX2, TUBB3 & CHD7* but no change in *SOX10* and *SEMA3A*. However, by Day 21, a 2.4-fold increase in *SEMA3A* and 2-fold increase in MKRN3 expression levels had become evident (**Figure 3B**).

Discussion

LiWGS in a KS patient with a known *de novo* chromosomal rearrangement identified a novel disruption in the lncRNA, *RMST. RMST*'s association with neuronal development is based on its strong, early neuronal localization and expression in the Wnt and TGFβ/BMP rich domains of the embryonic dorsal forebrain [48]. In addition, RMST expression increases during critical stages of neuronal differentiation [49, 50] when it binds directly to *SOX2 (23,61)*, a critical transcriptional regulator of GnRH ontogeny. *RMST* knock-downs in neuronal stem cells also reduce expression of *CHD7, SEMA3,* and *TUBB3* – all validated IGD-causing genes [51-53]. However, the biology of lncRNAs

in general and *RMST* specifically remain largely unclear in part due to the lack of any functional assay to assess their loss of function. Thus, to address the potential role of *RMST* depletion in our KS patient, we generated iPSC and NCC from this unique KS patient with a translocation-disrupting deletion in *RMST*.

RMST expression increases during normal neuronal differentiation and binds directly to and potentially amplifies *SOX2* and likely *SOX10's* effects on early GnRH neuronal development. In contrast, in the presence of this translocation, *RMST* expression was significantly lower compared to healthy iPSC cells and the NCC development was severely disrupted. A large number of IGD-causing genes, particularly ones already identified to be *SOX2*-dependent and hence play a critical role in NCC development (e.g. *CHD7* and *TUBB3),* failed to develop in the *RMST*-deficient iPSC and NCC cells.

We hypothesize that *RMST* plays an essential role as a co-factor for *SOX2* (and presumably *SOX10)* in GnRH neuronal differentiation by binding to the promoter regions of several important neurogenic genes. These include many known IGD-causing genes (*FGFR1, TAC3, NROB1, LEPR, SOX10, RNF216, OTUD4, FEZF1, MKRN3, MCM4, IL17RD* and *DUSP6). RMST* also shares binding with *SOX2* to the promoters of the same neurogenic transcription factor genes such as Neurogenin 2, underscoring its partnership with *SOX2*.

SOX2 has a known role in the early development of the hypothalamic-pituitary-gonadal axis and differentiation of GnRH neurons in addition among other neurogenic progenitors during development of olfactory and vomeronasal receptors [54]. Patients with heterozygous mutations in *SOX2* exhibit IGD with or without ocular defects [55]. Thus, the binding partners, *RMST* and *SOX2*, acting in concert oversee a common pathway of

downstream *SOX2*–dependent (and now '*RMST*-dependent') genes critical for GnRH neuronal differentiation as validated by the fact that most of these genes also cause KS when mutated [17, 21, 52, 53, 56].

RMST depletion led to initial decreases on Day 11 followed by further increases on Day 21 relative to controls in *MKRN3*, a paternally imprinted gene in the Prader-Willi/Angelman critical region whose LoF mutations are associated with precocious puberty (CPP) [57]. *Mkrn3* is highly expressed in the arcuate nucleus of the hypothalamus during the infantile and early juvenile periods with subsequent reductions at postnatal days 12-15, i.e. just prior to GnRH-induced sexual maturation in mice [57, 58]. Collectively, these observations suggest that *MKRN3* plays a 'braking' function in the pre-pubertal inhibition of GnRH secretion and that any sustained increase in its expression could lead to a potentially severe delay of pubertal development such as occurs in KS and IGD.

These associative data demonstrate for the first time that *RMST* is a lncRNA implicated in GnRH deficiency and has a key role as a co-governor with *SOX2* in regulating downstream KS genes, making it the potential cause of the KS phenotypic expression in our subject. It remains to be seen if other structural or genetic abnormalities in *RMST* and/or other non-coding genes in this domain (or others) can also cause KS. Future mammalian modeling e.g. *RMST* knock-outs will hopefully provide more detailed mechanistic and developmental insights into the mechanisms by which *RMST* governs GnRH neurogenesis. The previous inherent difficulties of examining functional consequence of alterations in non-coding regions has been a formidable generic limitation of studying mutations in this new class of disease-causing genes. However, the use of

IPSC and NCC cells begins to address these biological limitations in a convincing way, at least as *RMST* relates to neurogenesis and the ontogeny of GnRH neurons.

Even though rare *RMST* variants were discovered in both KS and nIHH patients, rare variants were also found in excess in control population. Given the non- coding nature of the gene, the functional effect of these point variants can be difficult to be examined. The rarity of KS (1:30,000 in men; 1:125,000 in women) [59], challenges efforts to seek replication of these findings in other humans. Importantly, no CNVs were detected in IGD cohort of 1,386 probands and no CNVs were detected in a large cohort of controls either (N=13,991), highlighting the rarity of occurrence of structural events in this genomic region. Similarly, structural defects causing human disease are rare but quite critical in revealing novel biological roles in such areas as autism. Thus, given the large body of coherent biologic evidence from these current studies, we believe these observations from this single KS patient lacking any other cause of his disease by WGS are coherent and call attention to a novel role of a LncRNA, *RMST,* as a genomic region worthy of further study. Future accurate WGS will continue to resolve ever smaller potential defects in other coding and non-coding genomic regions in important human disease models like IGD with relevance to developmental biology and pathophysiology.

The complexity of analyzing the genetic changes in noncoding areas led to identification of additional studies that implicated *RMST* to pubertal regulation. An association between the SNP rs76369685 located in the second intron of *RMST* and the age of menarche in the UK Biobank was detected [60]. The same SNP was also associated with gestational and type 1 diabetes in databases of 102,000 and 146,000 individuals (data not shown). Those associations highlight the importance of the intronic regions of this lncRNA and

can explain the lack of enrichment of exonic *RMST* genetic changes in the IGD cohort compared to controls.

In conclusion, *RMST's* high expression during normal neural crest cell differentiation, its direct association with key neural transcription factors, *SOX2* and *SOX10*, its ability to regulate downstream genes that control the reproductive axis such as *CHD7*, *TUBB3* and *MKRN3* and its association with the age of menarche all support a previously unappreciated role for *RMST* as a regulator of neural crest development potentially affecting GnRH precursors.

Authors contributions:

WFC, LWS, & MIS conceived and designed the study, participated in coordination, molecular genetics, data analyses and drafting the manuscript; SYN generated the NCC lines, performed the functional studies on them including Chip-seq, biochemistry, RIP, and participated in the manuscript drafting; HB performed molecular studies including liWGS and CNV analyses and participated in the manuscript drafting; HZW: analyzed CNV data; LP: performed/oversaw Sanger confirmations and molecular studies, WES and WGS analyses, and drafting the manuscript; LGB phenotyped and cared for the patient, oversaw all consenting of pedigree members, and participated in drafting the manuscript; SH: generated the patient-specific iPSC line; MLH & KCC: participated in design, execution and data analysis of targeted *RMST* sequencing in IGD cohort; RB & MET: participated in the experimental design, coordination of the molecular genetics and drafting of manuscript. JG: participated in analysis of the genetic translocation as part of the DGAP project. All authors read and approved the final manuscript.

Acknowledgements

Funded by NIH grants P50HD028138, R01HD081256, GM061354 and K99DE026824 and Singapore's Agency for Science, Technology and Research. Dr. Talkowski was supported as the Desmond and Ann Heathwood MGH Research Scholar. Dr. Stamou was funded by the Daland Fellowship of the American Philosophical Society. We thank the surviving patient family members who generously provided permissions to perform these studies. The DGAP project was supported by GM061354.

Conflict of Interest: None.

References:

1. Belchetz, P.E., et al., *Hypophysial responses to continuous and intermittent delivery of hypopthalamic gonadotropin-releasing hormone.* Science, 1978. **202**(4368): p. 631-3.
2. Stamou, M.I., K.H. Cox, and W.F. Crowley, Jr., *Discovering Genes Essential to the Hypothalamic Regulation of Human Reproduction Using a Human Disease Model: Adjusting to Life in the "-Omics" Era.* Endocr Rev, 2015. **2016**(1): p. 4-22.
3. Schwanzel-Fukuda, M. and D.W. Pfaff, *Origin of luteinizing hormone-releasing hormone neurons.* Nature, 1989. **338**(6211): p. 161-4.
4. Wray, S., P. Grant, and H. Gainer, *Evidence that cells expressing luteinizing hormone-releasing hormone mRNA in the mouse are derived from progenitor cells in the olfactory placode.* Proc Natl Acad Sci U S A, 1989. **86**(20): p. 8132-6.
5. Whitlock, K.E., et al., *Development of GnRH cells: Setting the stage for puberty.* Molecular and cellular endocrinology, 2006. **254-255**: p. 39-50.
6. Forni, P.E., et al., *Neural crest and ectodermal cells intermix in the nasal placode to give rise to GnRH-1 neurons, sensory neurons, and olfactory ensheathing cells.* The Journal of neuroscience : the official journal of the Society for Neuroscience, 2011. **31**(18): p. 6915-27.
7. Schlosser, G., *Making senses development of vertebrate cranial placodes.* Int Rev Cell Mol Biol, 2010. **283**: p. 129-234.
8. Pingault, V., et al., *Loss-of-function mutations in SOX10 cause Kallmann syndrome with deafness.* Am J Hum Genet, 2013. **92**(5): p. 707-24.
9. Bick, D., et al., *Male infant with ichthyosis, Kallmann syndrome, chondrodysplasia punctata, and an Xp chromosome deletion.* American journal of medical genetics, 1989. **33**(1): p. 100-7.
10. Schwanzel-Fukuda, M., et al., *Migration of luteinizing hormone-releasing hormone (LHRH) neurons in early human embryos.* J Comp Neurol, 1996. **366**(3): p. 547-57.
11. Ballabio, A., et al., *X-linked ichthyosis, due to steroid sulphatase deficiency, associated with Kallmann syndrome (hypogonadotropic hypogonadism and anosmia): linkage relationships with Xg and cloned DNA sequences from the distal short arm of the X chromosome.* Human genetics, 1986. **72**(3): p. 237-40.
12. Petit, C., J. Levilliers, and J. Weissenbach, *Long-range restriction map of the terminal part of the short arm of the human X chromosome.* Proc Natl Acad Sci U S A, 1990. **87**(10): p. 3680-4.
13. Franco, B., et al., *A gene deleted in Kallmann's syndrome shares homology with neural cell adhesion and axonal path-finding molecules.* Nature, 1991. **353**(6344): p. 529-36.
14. Vermeulen, S., et al., *Kallmann syndrome in a patient with congenital spherocytosis and an interstitial 8p11.2 deletion.* Am J Med Genet, 2002. **108**(4): p. 315-8.
15. Dode, C., et al., *Novel FGFR1 sequence variants in Kallmann syndrome, and genetic evidence that the FGFR1c isoform is required in olfactory bulb and palate morphogenesis.* Human mutation, 2007. **28**(1): p. 97-8.
16. Kim, H.G., et al., *WDR11, a WD protein that interacts with transcription factor EMX1, is mutated in idiopathic hypogonadotropic hypogonadism and Kallmann syndrome.* American journal of human genetics, 2010. **87**(4): p. 465-79.

17. Young, J., et al., *SEMA3A deletion in a family with Kallmann syndrome validates the role of semaphorin 3A in human puberty and olfactory system development.* Human reproduction, 2012. **27**(5): p. 1460-5.
18. Talkowski, M.E., et al., *Clinical diagnosis by whole-genome sequencing of a prenatal sample.* N Engl J Med, 2012. **367**(23): p. 2226-32.
19. Talkowski, M.E., et al., *Sequencing chromosomal abnormalities reveals neurodevelopmental loci that confer risk across diagnostic boundaries.* Cell, 2012. **149**(3): p. 525-37.
20. Redin, C., et al., *The genomic landscape of balanced cytogenetic abnormalities associated with human congenital anomalies.* Nat Genet, 2017. **49**(1): p. 36-45.
21. Ng, S.Y., et al., *The long noncoding RNA RMST interacts with SOX2 to regulate neurogenesis.* Mol Cell, 2013. **51**(3): p. 349-59.
22. Best, L.G., et al., *Chromosome abnormality in Kallmann syndrome.* Am J Med Genet, 1990. **35**(3): p. 306-9.
23. Higgins, A.W., et al., *Characterization of apparently balanced chromosomal rearrangements from the developmental genome anatomy project.* Am J Hum Genet, 2008. **82**(3): p. 712-22.
24. Talkowski, M.E., et al., *Next-generation sequencing strategies enable routine detection of balanced chromosome rearrangements for clinical diagnostics and genetic research.* Am J Hum Genet, 2011. **88**(4): p. 469-81.
25. Brand, H., et al., *Cryptic and complex chromosomal aberrations in early-onset neuropsychiatric disorders.* Am J Hum Genet, 2014. **95**(4): p. 454-61.
26. Hanscom, C. and M. Talkowski, *Design of large-insert jumping libraries for structural variant detection using Illumina sequencing.* Curr Protoc Hum Genet, 2014. **80**: p. 7 22 1-9.
27. Brand, H., et al., *Paired-Duplication Signatures Mark Cryptic Inversions and Other Complex Structural Variation.* Am J Hum Genet, 2015. **97**(1): p. 170-6.
28. Collins, R.L., et al., *Defining the diverse spectrum of inversions, complex structural variation, and chromothripsis in the morbid human genome.* Genome Biol, 2017. **18**(1): p. 36.
29. Stamou, M., et al., *Supplementary appendix.* Dataset posted on 16.05.2019, 22:06 by, 2019.
30. Stamouli, S., et al., *Copy Number Variation Analysis of 100 Twin Pairs Enriched for Neurodevelopmental Disorders.* Twin Res Hum Genet, 2018. **21**(1): p. 1-11.
31. Logue, M.W., et al., *The Psychiatric Genomics Consortium Posttraumatic Stress Disorder Workgroup: Posttraumatic Stress Disorder Enters the Age of Large-Scale Genomic Collaboration.* Neuropsychopharmacology, 2015. **40**(10): p. 2287-97.
32. Harrow, J., et al., *GENCODE: the reference human genome annotation for The ENCODE Project.* Genome Res, 2012. **22**(9): p. 1760-74.
33. Mica, Y., et al., *Modeling neural crest induction, melanocyte specification, and disease-related pigmentation defects in hESCs and patient-specific iPSCs.* Cell Rep, 2013. **3**(4): p. 1140-52.
34. Chambers, S.M., et al., *Combined small-molecule inhibition accelerates developmental timing and converts human pluripotent stem cells into nociceptors.* Nat Biotechnol, 2012. **30**(7): p. 715-20.

35. Feng, J., et al., *Identifying ChIP-seq enrichment using MACS.* Nat Protoc, 2012. **7**(9): p. 1728-40.
36. Heinz, S., et al., *Simple combinations of lineage-determining transcription factors prime cis-regulatory elements required for macrophage and B cell identities.* Mol Cell, 2010. **38**(4): p. 576-89.
37. Lek, M., et al., *Analysis of protein-coding genetic variation in 60,706 humans.* Nature, 2016. **536**(7616): p. 285-91.
38. Kaiser, P., *Pericentric inversions. Problems and significance for clinical genetics.* Hum Genet, 1984. **68**(1): p. 1-47.
39. Hsu, L.Y., et al., *Chromosomal polymorphisms of 1, 9, 16, and Y in 4 major ethnic groups: a large prenatal study.* Am J Med Genet, 1987. **26**(1): p. 95-101.
40. Teo, S.H., et al., *Pericentric inversion 9--incidence and clinical significance.* Ann Acad Med Singapore, 1995. **24**(2): p. 302-4.
41. Yamada, K., *Population studies of INV(9) chromosomes in 4,300 Japanese: incidence, sex difference and clinical significance.* Jpn J Hum Genet, 1992. **37**(4): p. 293-301.
42. Kim, J.J., et al., *Prenatal detection of de novo inversion of chromosome 9 with duplicated heterochromatic region and postnatal follow-up.* Exp Mol Med, 1999. **31**(3): p. 134-6.
43. Chan, A.S., et al., *Identification of a novel gene NCRMS on chromosome 12q21 with differential expression between rhabdomyosarcoma subtypes.* Oncogene, 2002. **21**(19): p. 3029-37.
44. MacDonald, J.R., et al., *The Database of Genomic Variants: a curated collection of structural variation in the human genome.* Nucleic Acids Res, 2014. **42**(Database issue): p. D986-92.
45. Adzhubei, I.A., et al., *A method and server for predicting damaging missense mutations.* Nat Methods, 2010. **7**(4): p. 248-9.
46. Kumar, P., S. Henikoff, and P.C. Ng, *Predicting the effects of coding non-synonymous variants on protein function using the SIFT algorithm.* Nat Protoc, 2009. **4**(7): p. 1073-81.
47. Jiang, Y., M.P. Epstein, and K.N. Conneely, *Assessing the impact of population stratification on association studies of rare variation.* Hum Hered, 2013. **76**(1): p. 28-35.
48. Caronia-Brown, G., A. Anderegg, and R. Awatramani, *Expression and functional analysis of the Wnt/beta-catenin induced mir-135a-2 locus in embryonic forebrain development.* Neural Dev, 2016. **11**: p. 9.
49. Uhde, C.W., et al., *Rmst is a novel marker for the mouse ventral mesencephalic floor plate and the anterior dorsal midline cells.* PLoS One, 2010. **5**(1): p. e8641.
50. Hart, R.P. and L.A. Goff, *Long noncoding RNAs: Central to nervous system development.* Int J Dev Neurosci, 2016. **55**: p. 109-116.
51. Chew, S., et al., *A novel syndrome caused by the E410K amino acid substitution in the neuronal beta-tubulin isotype 3.* Brain : a journal of neurology. **136**(Pt 2): p. 522-35.
52. Hanchate, N.K., et al., *SEMA3A, a Gene Involved in Axonal Pathfinding, Is Mutated in Patients with Kallmann Syndrome.* PLoS genetics, 2012. **8**(8): p. e1002896.
53. Kim, H.G., et al., *Mutations in CHD7, encoding a chromatin-remodeling protein, cause idiopathic hypogonadotropic hypogonadism and Kallmann syndrome.* Am J Hum Genet, 2008. **83**(4): p. 511-9.

54. Tucker, E.S., et al., *Proliferative and transcriptional identity of distinct classes of neural precursors in the mammalian olfactory epithelium.* Development, 2010. **137**(15): p. 2471-81.
55. Kelberman, D., et al., *Mutations within Sox2/SOX2 are associated with abnormalities in the hypothalamo-pituitary-gonadal axis in mice and humans.* J Clin Invest, 2006. **116**(9): p. 2442-55.
56. Chew, S., et al., *A novel syndrome caused by the E410K amino acid substitution in the neuronal beta-tubulin isotype 3.* Brain : a journal of neurology, 2013. **136**(Pt 2): p. 522-35.
57. Abreu, A.P., et al., *A new pathway in the control of the initiation of puberty: the MKRN3 gene.* J Mol Endocrinol, 2015. **54**(3): p. R131-9.
58. Abreu, A.P., et al., *Loss-of-function mutations in the genes encoding prokineticin-2 or prokineticin receptor-2 cause autosomal recessive Kallmann syndrome.* J Clin Endocrinol Metab, 2008. **93**(10): p. 4113-8.
59. Laitinen, E.M., et al., *Incidence, phenotypic features and molecular genetics of Kallmann syndrome in Finland.* Orphanet journal of rare diseases, 2011. **6**: p. 41.
60. Kichaev, G., et al., *Leveraging Polygenic Functional Enrichment to Improve GWAS Power.* Am J Hum Genet. **104**(1): p. 65-75.
61. Christian A. Koch,Vetta Vedanarayanan. Micropenis SOX. Poster Board Number: SAT-461. 97th Endocrine Society meeting. March 7, 2015, San Diego.

Table 1: Rare sequencing variants (RSVs) in ***RMST***.

Table 1 shows all the rare sequencing variants (RSVs) (defined as variants with allele frequenting <0.1% the gnomAD database) including their: chromosomal position, nucleic acid change, annotations (only the splice region changes have been annotated), exonal position, diagnosis of the affected proband, RSVs in other IGD genes. Note that all RSVs were found to be in heterozygous state.

Table 2: Burden testing in IGD vs. gnomAD cohort

Legend: Table 2 shows the prevalence of rare variation (MAF<1%) and very rare variation (MAF <0.1%) in the IGD cohort and the reference- control database of the gnomAD. The statistical differences were calculated between cohort of similar genetic background. MAF: minor allele frequency; N/A: not available.

Table 3: *SOX2* binding sites in known IGD genes and changes after depletion of *RMST*.

T**able 3** shows the *SOX2* binding sites of the known IGD genes. From the 35 known IGD genes, 15 contain a *SOX2* binding site. Upon deletion of *RMST* the *SOX2* binding sites disappear in 12 out of 15 genes including *FGFR1, TAC3*, *NROB1*, *LEPR*, *SOX10*, *RNF216, OTUD4, FEZF1*, *MKRN3, MCM4, IL17RD* and *DUSP6*. On the other hand, *SOX2* binding sites of *TACR3, TUBB3* and *FLRT3* were not altered upon deletion of *RMST* and one, *PROKR2,* gained one *SOX2* binding site.

Figure Legends:

Figure 1: Base pair resolution of the "balanced" chromosomal rearrangement demonstrates a breakpoint to be in *RMST*.

Figure 2: *RMST* levels in both the KS patient's IPSC (KS1) & healthy control's iPSCs; the patient's iPSCs expressed only 6%-18% of the total *RMST* transcripts (AK056164, AF429305 and AF429306) that were expressed by healthy iPSCs but with no significant differences in *SOX2* and *SOX10* expression in both cell lines.

Figure 3 A&B: Expression of *SOX2, SOX10, RMST* transcripts (AK056164, AF429305 & AF429306), *PAX3, GNRH1, TFAP2A, CHD7, SEMA3A, MKRN3* and *TUBB3* in patient's neural crest cells compared to controls after induction of NC differentiation for Days 11 and 21. KS1: patient's cells and CTS: control's cells.

Figure 4: Interaction of *RMST* transcripts AK056164 and AF429305 with *SOX2* and *SOX10*: RNA-immunoprecipitation was performed with isotype IgG as negative control and *SOX2* as positive control. Significant enrichment of *RMST* transcripts AK056164 and AF429305 in *SOX10* pulldown samples indicated interaction between *SOX10* and *RMST*.

Figure 5: *RMST* transcript quantification was repeated again on Day 11 of differentiation, when the iPSCs have differentiated into neural crest cells (NCS). Patient NC cells expressed <20% of the *RMST* transcripts present in healthy NC. KS1: patient's cells and CTS: control's cells.

Abbreviations: IGD- Isolated GnRH Deficiency, KS: Kallmann Syndrome, LiWGS: Long Insert Whole Genome Sequencing, NGS: Next Generation Sequencing, LncRNA: Long-non-coding RNA, KS1: NCC: Neural crest cells.

Table 1

Chr	bp	Ref	Alt	Annotation	Location	Dx	Gender	Other genes	Zygosity	gnomAD
12	97858842	A	G		Exon 1	KS	male	KLB c.820A>G p.I274V het; FGFR1 c.1097C>T p.P366L het	het	3.23E-05
12	97858843	T	C		Exon 1	nIHH	male		het	not seen
12	97885730	G	A		Exon 1 of MIR1251	KS	male		**hom**	not seen
12	97887656	T	A		Exon 5	KS	male	KAL1 c.1759G>T p.V587L hem	het	3.23E-05
12	97887663	G	A	n.256-6G>A	Exon 5	nIHH	male		het	0.000226
12	97887706	T	A		Exon 5	nIHH	male		het	not seen
12	97887763	G	A		Exon 5	KS	male		het	3.23E-05
12	97888490	C	T		Exon 6				het	0.00097
12	97888657	A	G	n.1521A>G	Exon 6				het	0.000807
12	97927340	T	C		Exon 9	KS	male		het	0.000486
12	97889772	C	A		Exon 7	KS	male		het	0.000129

12	97926848	C	T		Exon 9	KS	male	PROKR2 c.254G>A p.R85H het;	het	0.000388
12	97926848	C	G		Exon 9	KS	male		het	not seen
12	97962885	G	A		Exon 9	nIHH	female	IL17RD c.1697C>T p.P566L het;	het	not seen
						nIHH	male		het	
						KS	male	OTUD4 c.755T>C p.V252A het;	het	
						nIHH	male	CHD7 c.2831G>A p.R944H het; PROKR2 c.991G>A p.V331M het; FGFR1 c.289G>A p.G97S het	het	
						nIHH	male		het	

						KS	male	KLB c.1825A>G p.T609A het	het	
						nIHH	female	NR0B1 c.376G>A p.V126M het; PROK2 c.218G>A p.R73H het	het	
						nIHH	male	CHD7 c.120A>C p.Q40H het; CHD7 c.4565A>T p.D1522V het; PROKR2 c.949G>C p.V317L het	het	

12	97927223	C	T		Exon 9	KS	male	KAL1 c.1056_1060delGGATG p.T352TfsX2 hem; CHD7 c.8416C>G p.L2806V het;	het	0.000259
						nIHH	male		het	

Table 2

Chr	bp	Ref	Alt	Annotation	Location	Daignosis	Gender
12	97858842	A	G		Exon 1	KS	male
12	97858843	T	C		Exon 1	nIHH	male
12	97886308	G	C		Exon 3	KS	male
						KS	female
12	97887656	T	A		Exon 5	KS	male
12	97887663	G	A	n.256-6G>A	Exon 5	nIHH	male
12	97887706	T	A		Exon 5	niHH	male
12	97887763	G	A		Exon 5	KS	male
12	97888490	C	T		Exon 6	KS	male
12	97888657	A	G	n.1521A>G	Exon 6		
12	97927340	T	C		Exon 9		
12	97889772	C	A		Exon 7	KS	male
12	97926773	G	T		Exon 9	nIHH	male
						nIHH	male
12	97926848	C	T		Exon 9	KS	male
12	97926848	C	G		Exon 9	KS	male
12	97962885	G	A		Exon 9	nIHH	female
						nIHH	male
						KS	male
						nIHH	male
						nIHH	male
						KS	male
						nIHH	female

						nIHH	male
12	97927223	C	T		Exon 9	KS	male
						nIHH	male
12	17489-9792	GC	G		Exon 9	nIHH	female
						KS	male
						nIHH	male
						nIHH	male
						nIHH	male
						nIHH	male
						nIHH	male

Additional features	Other genes	Ethnicity
	KLB c.820A>G p.I274V het; FGFR1 c.1097C>T p.P366L het;	Asian
		Caucasian
External ear defect		Not assessed
Eye defects, speech impairement & cerebellar ataxia		Asian
Synkinesia	KAL1 c.1759G>T p.V587L hem	Caucasian
No		Caucasian
No		Caucasian
No		Not assessed
No		African american
Flat feet, kyphosis & hypermobility		Caucasian
No		Caucasian
Flat fett and eye defects	GLCE c.427G>A p.V143M het; POLR3B c.1-1C>T het; CHD7 c.7315G>A p.E2439K het; PNPLA6 c.1484C>T p.P495L het;	Caucasian
Deviated spectum & high arched palate	PROKR2 c.254G>A p.R85H het	Caucasian
Clinodactyly & neurologic defects		Asian
CL/CP	IL17RD c.1697C>T p.P566L het;	African American
No		Not assessed
Flat feet & pectus exvacatum	OTUD4 c.755T>C p.V252A het;	Asian
No	CHD7 c.2831G>A p.R944H het; PROKR2 c.991G>A p.V331M het; FGFR1 c.289G>A p.G97S het;	Asan
Ataxia		Not assessed
Synkinesia	KLB c.1825A>G p.T609A het;	Asian
No	PROK2 c.218G>A p.R73H het;	Asian

Crowded teeth & protruding ears	CHD7 c.120A>C p.Q40H het; CHD7 c.4565A>T p.D1522V het; PROKR2 c.949G>C p.V317L het;	Caucasian
Excessive joint mobility, high arched palate, synkinesia	KAL1 c.1056_1060delGGATG p.T352TfsX2 hem; CHD7 c.8416C>G p.L2806V het;	Not assessed
No		Caucasian
No	TACR3 c.623G>A p.W208X het;	Caucasian
Curved spine, foreshortened arm/leg & bone deformities	CHD7 c.5051-4C>T het; LEPR c.2246T>C p.L749S het; FGFR1 c.745+7G>A het; FGFR1 c.1809C>A p.C603X het;	Caucasian
No	GNRHR c.892_893insA p.N298KfsX22 hom; KISS1R c.998C>T p.A333V het;	Caucasian
No	IL17RD c.2012C>T p.S671L het; POLR3B c.543A>C p.Q181H het;	Caucasian
No		Caucasian
No		Caucasian
No	CHD7 c.2819C>T p.P940L het; also WES data not back	Caucasian

GnomAD MAF based in subpopulation ethnicity
None
None
0.003094 (East Asian)
None
None
0.0002665 (Non Finish Europeans); 0.0002862 (Finish Europeans)
None
0.00006666 (non Finish European)
0.003212
0.002749
0.001375
0.0002667
None
0.0006676 (non Finish European); 0.0002862 (Finish)
None
None

0.0003339 (Non Finish European); 0.0002862 (Finish Europeans); 0.001196 (Latino); 0.001018 (Other)
0.001671 (Non Finish Europeans); 0.0002864 (Finish Europeans)

Table 3

	SOX2 binding site
KAL1	No
NROB1(DAX1)	chrX:30237372:30237587
GNRHR	No
PCSK1	No
LEP	no
FGFR1	chr8:38444431:38445018
KISS1R	no
NSFM(NELF)	no
PROKR2	no
PROK2	no
LEPR	chr1:65658276:65658800
FGF8	no
CHD7	no
GNRH1	no
TAC3	chr12:55696425:55696910
TACR3	chr4:104859805:104860418
WDR11	no
HS6ST1	no
POLR3B	no
KISS1	no
SEMA3A	no
FGF17	no
IL17RD	chr3:57173766:57174183
SPRY4	no
DUSP6	chr12:88270267:88270887
FLRT3	chr20:14266025:14266376
SOX10	chr22:36709222:36709997
OTUD4	chr4:146320233:146320452
RNF216	chr7:5787630:5788029
TUBB3	chr16:88516780:88517669
FEZF1	chr7:121731148:121731552
PNPLA6	no
STUB1	no
AXL	no
MKRN3	chr15:21361791:21362052

SOX2 binding site (absence of *RMST*)
No
No
No
No
No
No
No
No
chr20:5243291:5244788
No
No
No
No
No
No
chr4:104859537:104861056
No
No
No
No
No
No
No
No
No
chr20:14265925:14266584
No
No
No
chr16:88517627:88518915
No
No
No
No
No

Figure 1

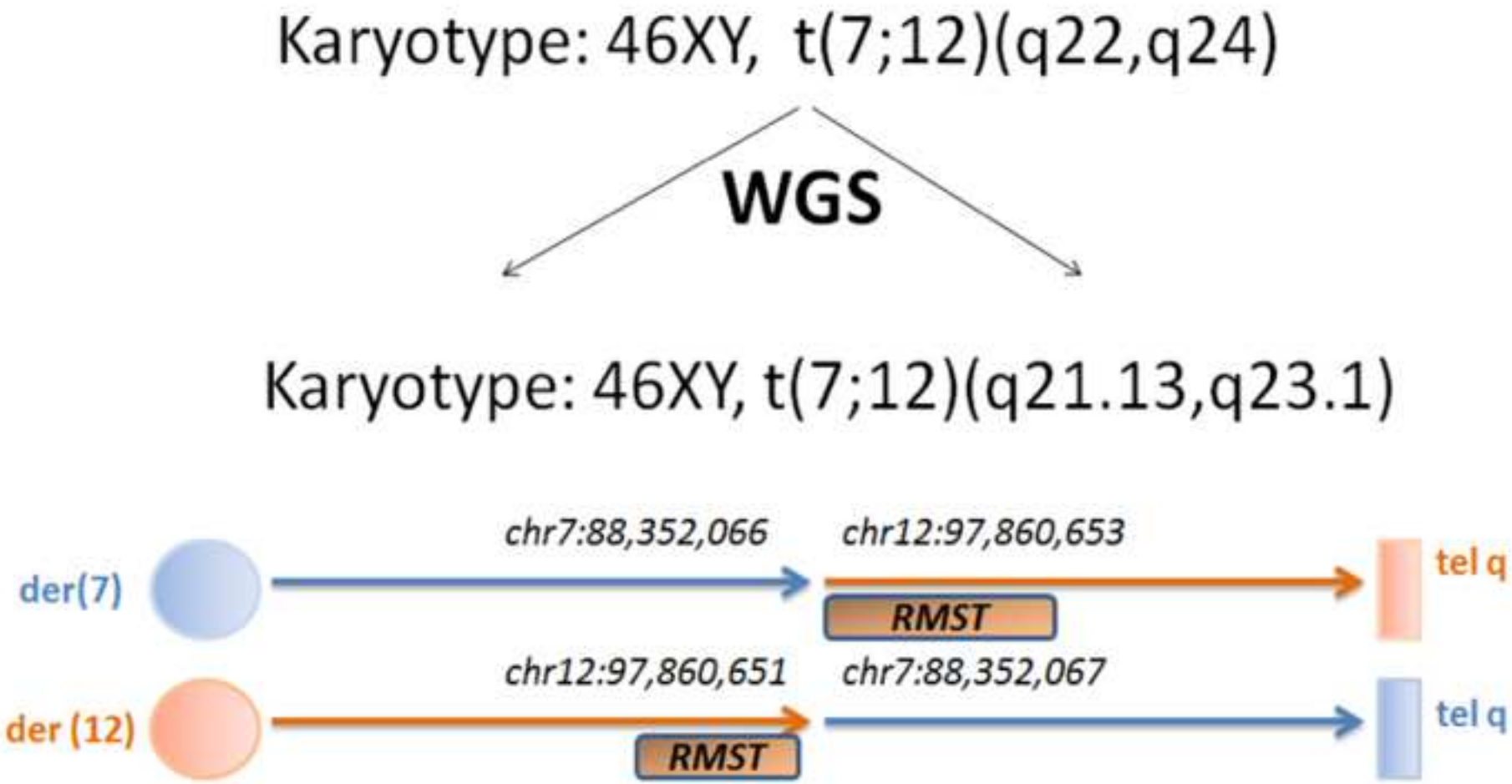

Figure 2: Expression of *SOX2*, *SOX10* and 3 transcripts of *RMST* in the patient's (KS1) vs control (CTS) IPS cells.

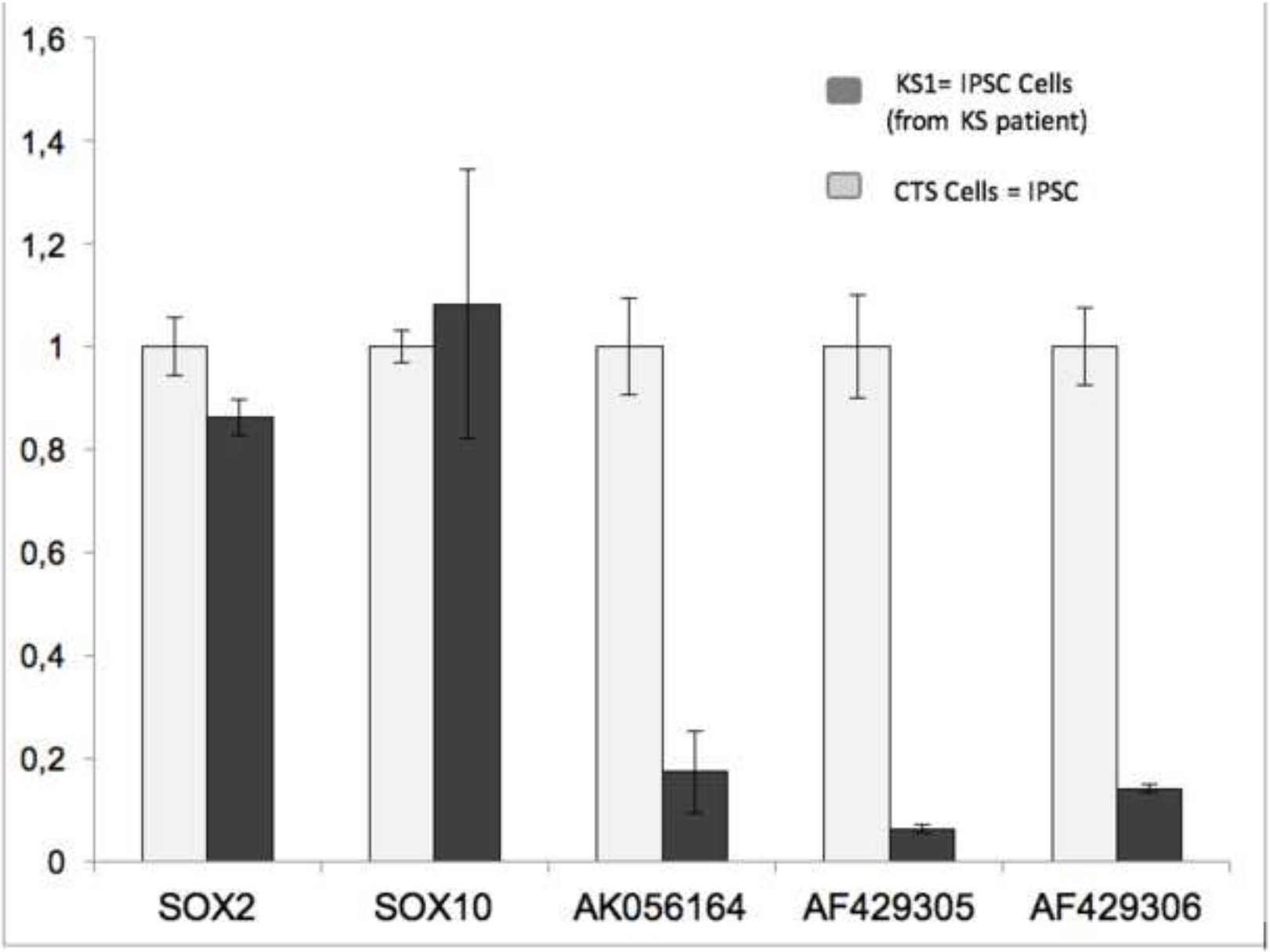

Figure 3A&B: Effect of RMST on known IGD genes.

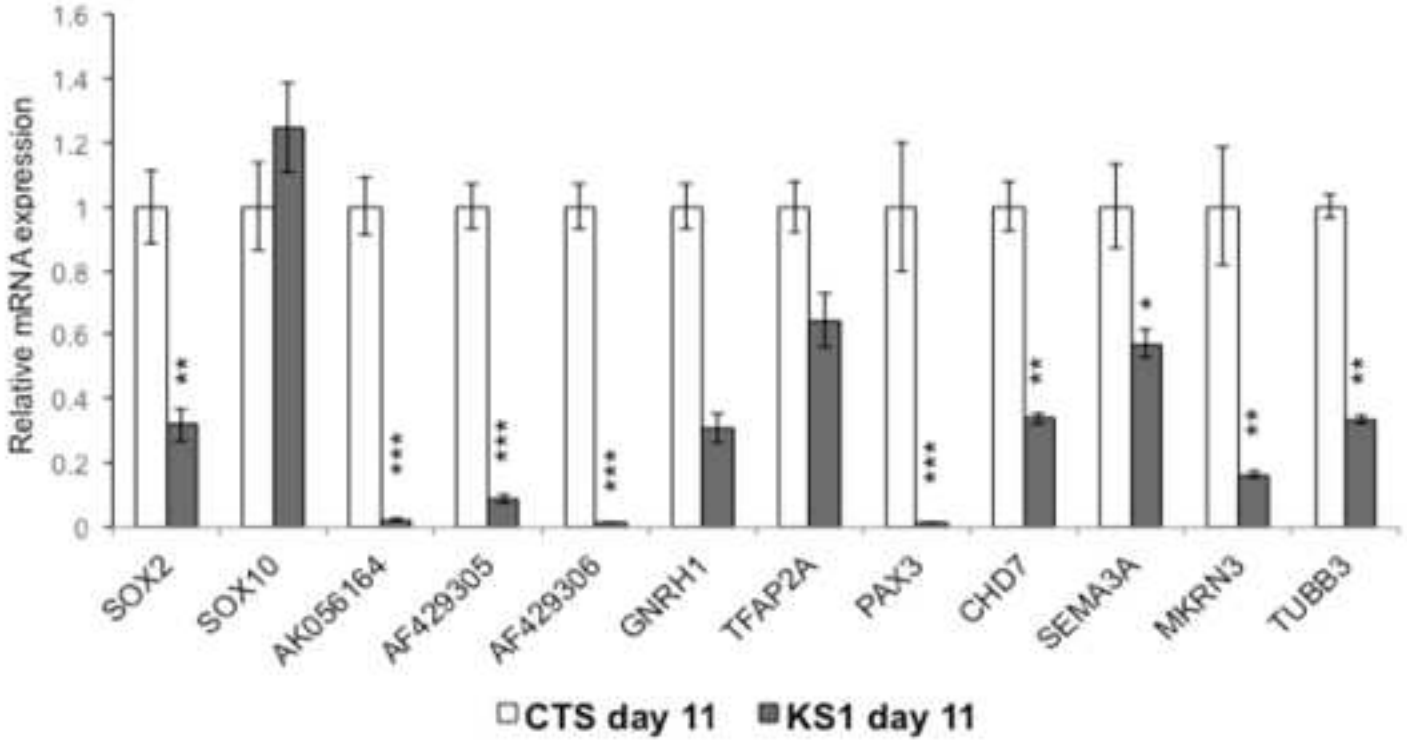

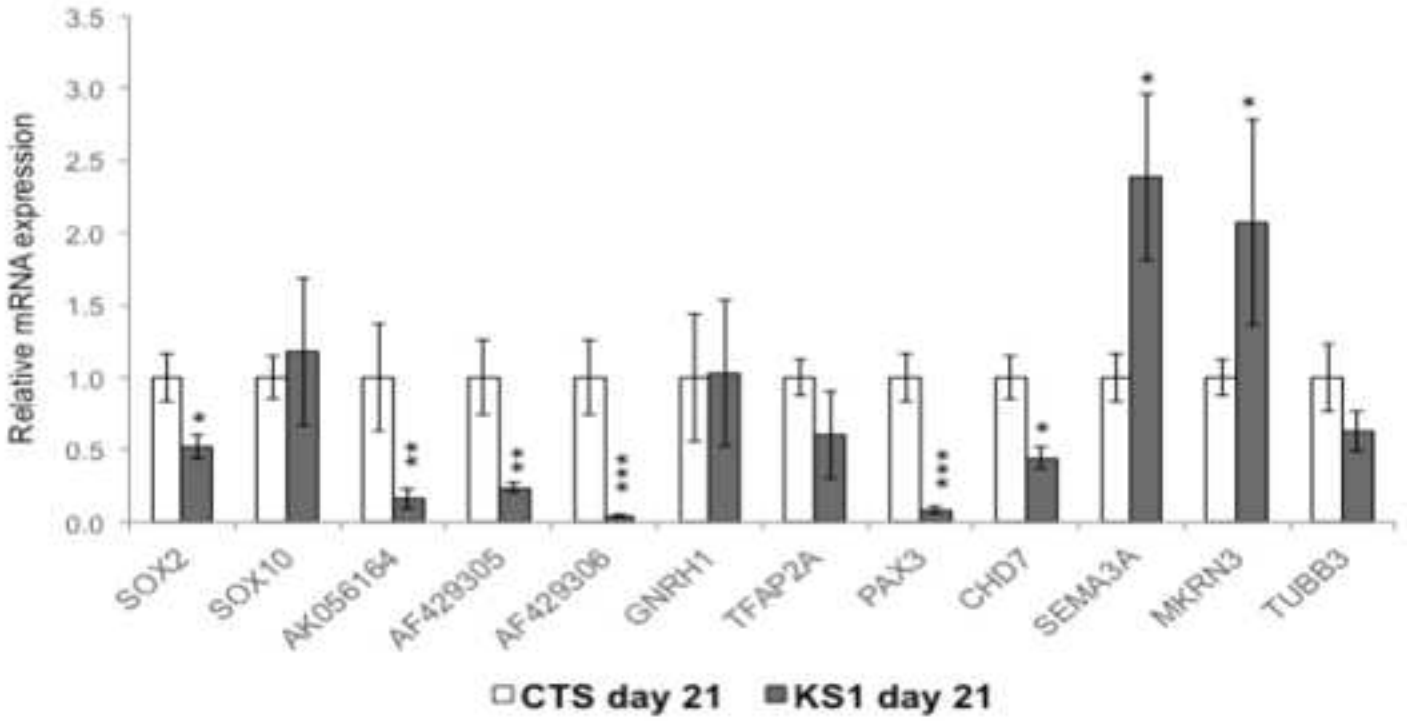

Figure 4: *RMST* interacts with *SOX10*.

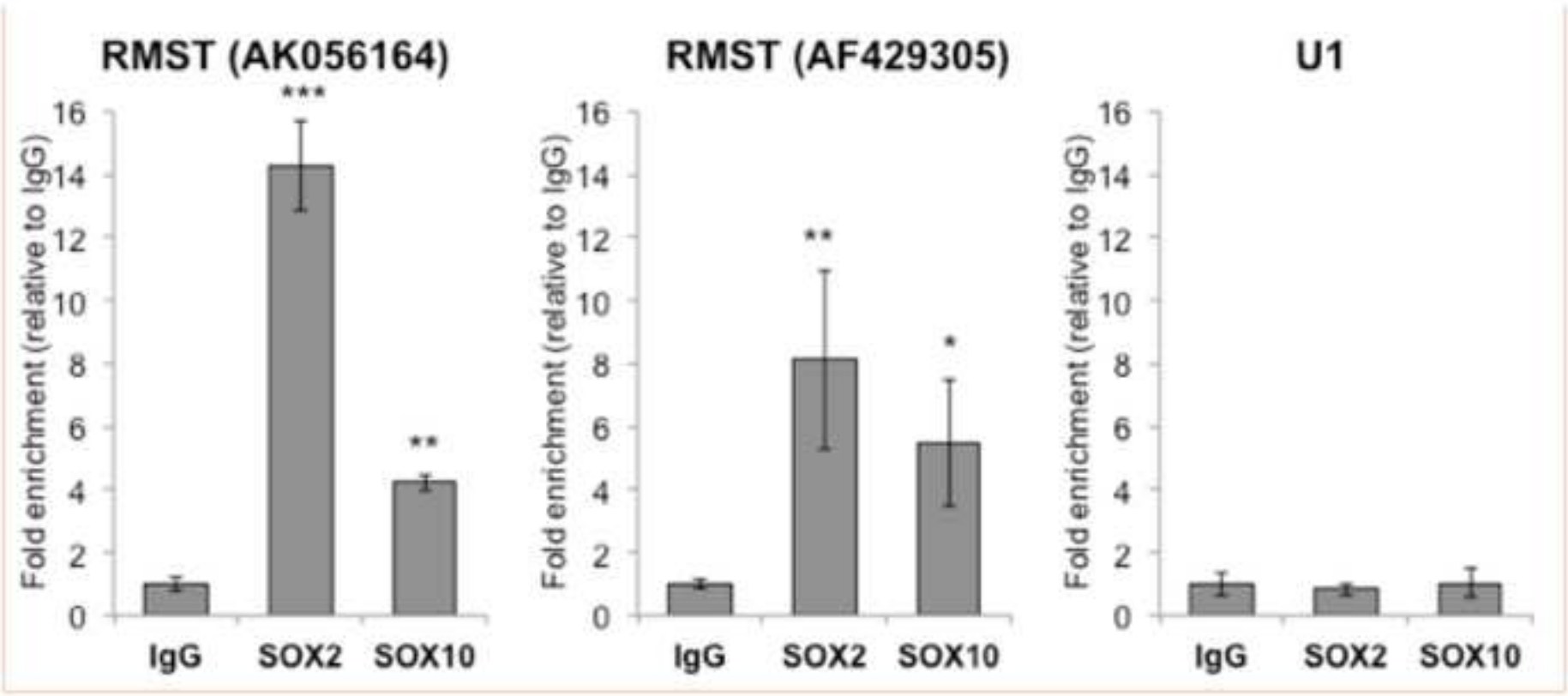

Figure 5: LCL-iPSC are less capable of neural crest differentiation than controls IPSCs.